Switching probability sub-distributions and asymmetric magnetization reversal in FePt nanostructures

L. Herrera Diez, A. Bernand-Mantel, L. Ranno, D. Givord

Institut Néel - CNRS-UJF, 25 avenue des Martyrs, F-38042 Grenoble Cedex 9, France

E-mail: liza.herreradiez@grenoble.cnrs.fr

L. Vila, P. Warin, A. Marty

INAC,SP2M, CEA Grenoble, 38054 Grenoble, France
Université Joseph Fourier, BP 53-38041

Abstract. The coercive field statistics in FePt nanostructures reveals the existence of multiple switching probability sub-distributions that can be asymmetric with respect to the field orientation. Each sub-distribution is correlated to an individual magnetization reversal path whose selection can not happen at the magnetization reversal in negative (positive) field but rather at the moment of applying the initial positive (negative) magnetic field. This serves to determine the reference magnetic state from which reversal in negative (positive) field will develop. The disappearance of the asymmetric sub-distributions upon increasing the initial magnetic field $\mu_0 H_{max}$ supports this model. However, the sub-distributions remaining at high $\mu_0 H_{max}$ are not necessarily those characterized by the highest coercive field. This is attributed to the fact that the initial magnetization state hierarchy and the coercive field hierarchy are essentially decorrelated.

The high uniaxial magnetic anisotropy in FePt[1, 2, 3] makes it a promising candidate for extending the current limits of magnetic recording densities without compromising the necessary thermal stability[4, 5, 6, 7, 8, 9, 10]. Driven by the interest in potential applications in perpendicular magnetic recording and bit-patterned media[11, 12] technologies this system has been the subject of various studies concerning magnetization reversal processes. The high efficiency of spin-transfer associated to the high perpendicular magnetic anisotropy makes the control of coercivity due to domain wall pinning a key point for the development of DW-propagation based memories and logic systems[13, 14, 15].

Field and current driven magnetic domain wall dynamics in FePt nanostructures have been examined focusing on thermally activated depinning processes. Domain wall depinning under applied magnetic fields investigated down to the single pinning defect limit was found to occur via a multiple path mechanism[16].

In this work, the coercive field statistics in FePt nanostructures is derived from magneto-transport and Kerr microscopy measurements. Multiple switching probability sub-distributions and asymmetric magnetization reversals are identified and shown to depend on the amplitude of the maximum positive (negative) initial magnetic field, $\mu_0 H_{max}$. This field is applied before studying the magnetization reversal in negative (positive) fields and serves to establish the magnetic state from which reversal develops.

The samples studied were 4 nm thick epitaxial FePt $L1_0$ films grown on Pt(001)(20 nm)/Cr (2nm)/MgO(001), further details regarding the material growth can be found in Ref.[17]. The films were capped with a 5 nm MgO layer and patterned into Hall bar structures by electron beam lithography. The main channel of the Hall bar structures was 500 nm wide and 10 μm long. All the magnetization loops were obtained by extraordinary Hall effect measurements using a bias current of 1 mA and a constant magnetic field rate of 0.1 T/min.

The positive and negative field switching probability distributions obtained at different temperatures are shown in Fig. 1 as a function of the applied magnetic field H_{ap} where $\mu_0 H_{max} = \pm 0.6$ T. The distributions have been determined from sets of 30 to 100 loops[18]. At 300 K the switching probability distributions found in both positive and negative fields can be described in terms of a single distribution function. In contrast, the measurements at 200 K show a splitting of the switching probability distribution for the reversal in positive fields with one sub-distribution between 0.26 T and 0.3 T and a second between 0.3 T and 0.34 T. The low field sub-distribution is absent for the reversal under negative fields revealing a marked switching field asymmetry. A similar scenario is found at 100 K where three sub-distributions are present for the reversal under negative fields and only one for the reversal under positive fields (see Fig. 1). Multiple sub-distributions as well as switching asymmetries were observed in all samples measured. The number of sub-distributions and the features characterizing the switching field asymmetry varied from sample to sample. Note that the shape of the switching probability distribution (number and position of symmetric/asymmetric sub-distributions) is independent from the polarity of the starting saturation field (namely,

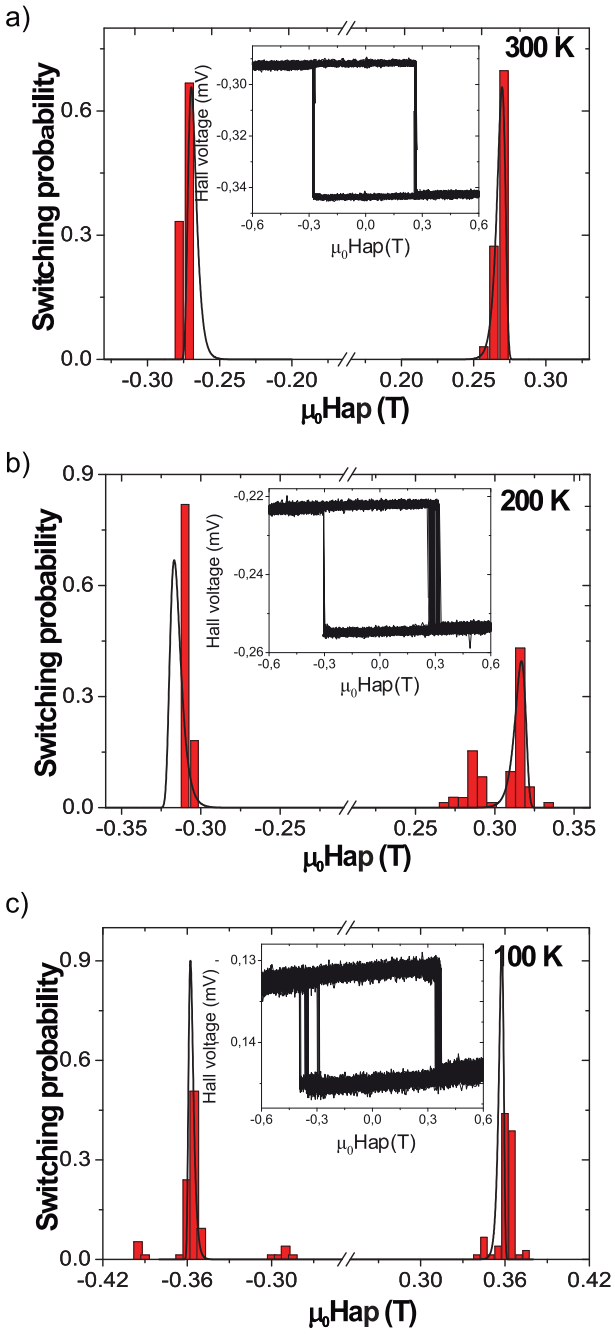

Figure 1. Switching probability distribution as a function of the applied magnetic field ($\mu_0 H_{max} = \pm$ 0.6T) at (a) 300 K, (b) 200 K and (c) 100 K. Multiple sub-distributions appear at lower temperatures where also a marked switching asymmetry is evidenced between positive and negative fields at 200 K and 100 K. A continuous line indicates an estimation of the switching probability (sub)distribution considering a model with a single energy barrier of 3.3×10^{-19} J. The magnetization loops corresponding to each switching probability distribution are shown in the insets.

no differences were found between starting from H_{max} or -H_{max}).

At 300 K, the single peak switching probability distribution resembles that

characterizing a magnetization reversal involving a single energy barrier. The energy barrier as a function of the magnetic field is expected to be ruled by the expression:

$$E = E_0(1 - \frac{H_{ap}}{H_0})^{\alpha} \tag{1}$$

where E_0 is the energy barrier in zero magnetic field and $\mu_0 H_0$ is the coercive field in the absence of thermal activation. The value of the exponent α depends on the coercivity mechanism. It ranges from 1 to 2, where $\alpha = 1$ accounts for reversals governed by domain wall nucleation/propagation and $\alpha = 2$ for ideally textured systems in which the magnetization reversal occurs by Stoner-Wohlfarth coherent rotation [19, 20, 21]. It is worth noting that a process involving overcoming an energy barrier leads necessarily to a nucleation event from which the process is triggered, regardless of the dominating micromagnetic process, namely, magnetic domain nucleation or domain wall pinning. The distinction between a domain nucleation and a domain wall pinning process will be discussed in the last part of this manuscript.

The characteristic switching time in a constant field is:

$$\tau = \tau_0 \exp[E/kT] \tag{2}$$

where τ_0 is a pre-exponential factor fairly independent of the magnetic field[22]. The mathematical expression accounting for the switching probability distribution in the whole field range $p(\mu_0 H_{ap})$ evaluates the product of the switching rate at a given applied field $\mu_0 H_{ap}$ multiplied by the probability of the magnetization reversal not having yet occurred (in the interval between 0 and $\mu_0 H_{ap}$) [23, 24, 25]:

$$p(\mu_0 H_{ap}) = (\tau v)^{-1} \exp[-\int_0^{\mu_0 H_{ap}} (\tau v)^{-1} d\mu_0 H_{ap}]. \tag{3}$$

where $v = \mu_0 dH_{ap}/dt = 0.1$ T/min. Eq. 3 was employed to model the measured switching probability distributions as shown in Fig. 1 (solid line). The parameters were optimized to account simultaneously for the experimental distribution functions for both positive and negative applied fields. The values obtained are $\alpha = 1$, $\tau_0 = 8{\times}10^{-11}$ s, $\mu_0 H_0 = 0.390$ T and $E_0 = 3.3{\times}10^{-19}$ J which is of the order of the zero field energies found in other FePt studies[16]. Except for a change from 0.390 to 0.399 in $\mu_0 H_0$ the curves at lower temperatures have been obtained with the same values of α, τ_0, and E_0. In the room temperature results the modeled peaks have the same area/amplitude for negative and positive applied fields since only one and the same distribution accounts for the entire switching probability for both polarities of the applied field. In the case of the the low temperature measurements it is the sum of the area of the sub-distributions that amounts to a switching probability of one. At low temperatures the model fits one of the multiple sub-distributions for each polarity of the applied magnetic field. In this case, given the asymmetry in the magnetization reversal, the amplitudes are allowed to differ.

Upon reducing the temperature the coercive field value $\mu_0 H_c$ at the center of the main (sub)distribution increases from 0.262 T at 300K to 0.314 T and 0.355 T at 200K and 100K, respectively. This common behaviour can be attributed to the usual increase in

magnetocrystalline anisotropy as well as to the reduction of thermal activation effects with decreasing temperature. Simultaneously, the difference between $\mu_0 H_c$ and $\mu_0 H_0$ significantly decreases ($\Delta\mu_0 H = \mu_0(H_0 - H_c)$, $\Delta\mu_0 H(300\text{K}) = 0.128$ T, $\Delta\mu_0 H(200\text{K}) = 0.085$ T, $\Delta\mu_0 H(100\text{K}) = 0.044$ T) accompanied by a reduction in the width of the distribution. The single energy barrier model successfully predicts the evolution of the distribution width as a function of temperature. Additionally, the (unique) distribution found at 300K corresponds to the sub-distribution of larger amplitude at lower temperatures. This can be observed in the positive switching probability distribution at 200 K and its negative field counterpart at 100 K. Therefore, a decrease in thermal energy allows for the observation of not only the magnetization reversal path present at 300 K but also of other reversal paths.

If the difference in the values of the energy barriers of two possible processes is small compared to the thermal energy a clear differentiation between the statistics of these two processes will not be observable. This may account for the single peak distribution found at 300K. As the temperature decreases, the switching field differences would start to show due to the decrease in thermal energy. However, the large differences (compared to the width of the sub-distributions) between the energy barriers estimated from the coercive field values ($E_0 = \mu_0 HMv$ where $v \approx d^3$ and d is the domain wall width) would not allow multiple processes to occur. Thus, we are led to conclude that the simultaneous appearance of multiple sub-distributions can not be explained using statistical arguments and that the sub-distributions reflect independent reversal paths that have a non-trivial correspondence with their respective coercive field values. This can be understood by considering that the selection of the reversal mechanism is determined at the moment of the creation of the initial magnetization state, namely, at the moment of the application of $\mu_0 H_{max}$.

The conclusion that the reversal path depends on the initial magnetization state, which is in turn determined by $\mu_0 H_{max}$, leads to investigate the dependence of the switching probability distribution on $\mu_0 H_{max}$. In Fig. 2 the positive field side of the switching probability distribution measured at 200 K (a) and the negative field side of the switching probability distribution at 100 K (b) are presented for two different values of $\mu_0 H_{max}$: ± 0.6 T (same plots as in Fig. 1) and $\pm$ 2 T. The asymmetric sub-distributions found for $\mu_0 H_{max} = 0.6$ T can be entirely suppressed by increasing to $\mu_0 H_{max}$ to 2 T. This is shown in Fig. 2 (a) for measurements at 200 K and in Fig. 2 (b) for measurements at 100 K.

Upon increasing $\mu_0 H_{max}$, it could have been expected that low field switching events would disappear. However, the asymmetric sub-distributions that disappear in high saturation field measurements can be centered at either higher or lower fields with respect to the symmetric sub-distributions, as shown in Fig. 2 (b): the initial magnetization state that prevails in a large saturation field is not necessarily the one that will lead to the highest coercive field. This shows that the initial magnetization state hierarchy does not have a one to one correspondence with the coercive field hierarchy. This behaviour confirms the decorrelation between the magnitude of H_{max} and that of the coercive field.

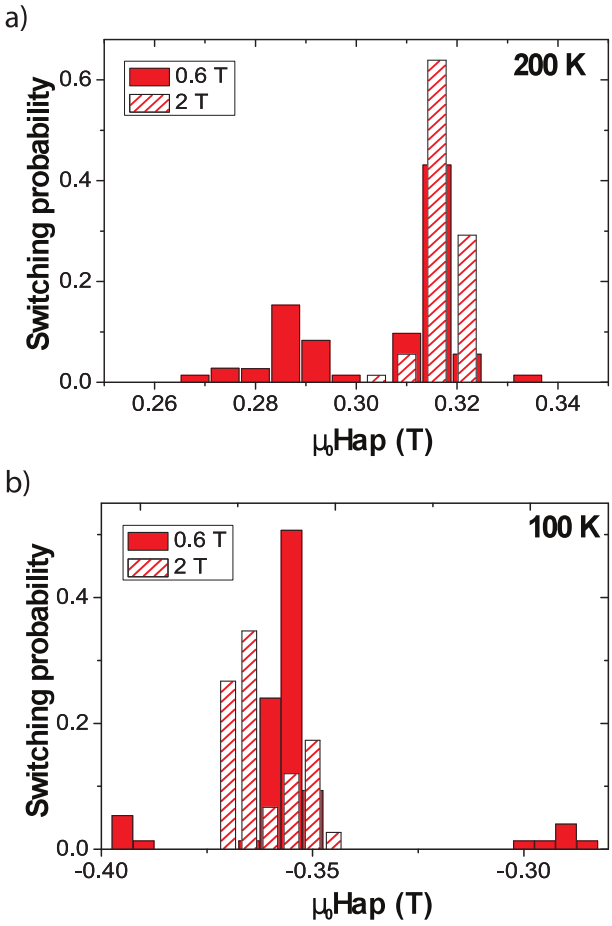

Figure 2. Positive field side of the switching probability distribution measured at 200 K (a) and negative field side of the switching probability distribution at 100 K (b) are presented for two different values of $\mu_0 H_{max}$: $\pm$0.6 T (same plots as in Fig. 1) and $\pm$ 2 T. At $\pm$ 2 T the switching probability distribution shows only one peak.

Such a decorrelation between initial applied field and coercive field is known to occur in the 'nucleation-type' hard magnets such a NdFeB. It is explained by considering that the reversal develops from a small preformed nucleus at the surface of the grains. There are several differences between eliminating a domain wall from a grain (to reach saturation) and propagating a domain wall inside a grain (to reverse its magnetization). The first of these differences is the intrinsic asymmetry of the coercive barrier. It is immediately apparent for a Stoner-Wolhfarth particle: the coercive field is equal to the anisotropy field whereas the field required to saturate a grain's magnetization is equal to the demagnetizing field of this grain. Another difference is in the value of the internal field which ultimately determine the magnetization processes. During the phase of saturation, the grain demagnetizing field is antiparallel to H_{ap}. During magnetization reversal both fields are parallel. In the case of the NdFeB magnets, there is ample experimental evidence that the same asymmetry in the coercive barrier exists[26, 27]. Extending this reasoning to the FePt films here considered, we suggest that pinning of domain walls

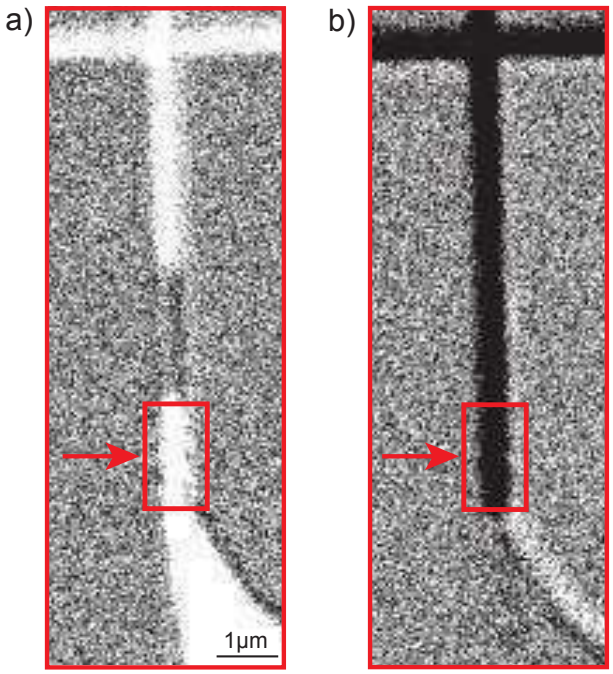

Figure 3. Kerr microscopy images at room temperature of a magnetic structure equivalent to that used for Hall measurements. Inside the highlighted area the magnetization is reversed in (a) by a domain wall coming from the contact pad and in (b) by a domain wall coming from the Hall cross.

occur at a few sites, which are intrinsically asymmetric. This, together with the above discussed effect of the demagnetizing field, provide the conditions for establishing different energy barrier hierarchies during sample saturation and magnetization reversal, respectively.

The possibility of switching the same magnetic unit via the propagation of domain walls generated at different sources (initial states), in turn giving rise to distinct switching probability sub-distributions, has been confirmed by Kerr microscopy. In these experiments the domain pattern has been observed after applying a pulsed magnetic field. In particular, the images in Fig. 3 (a) and (b) reveal two different intermediate states in the magnetization reversal at 300 K of a magnetic structure equivalent to that used for Hall measurements. These images show a domain wall mediated magnetization reversal involving 180° domain walls. The reversal has been observed to occur by the propagation of a few domain walls across the FePt nanostructure rather than by an extended pattern of small domains. The domain wall thickness is of the order of 4 nm, this value is defined by the strong uniaxial magnetic anisotropy in FePt which also explains the propagation dominated reversal typical of high anisotropy materials.[16]. The highlighted area shows a part of the magnetic structure where a segment of one of the 500 nm wide side channels is reversed in (a) by a domain wall coming from the contact pad and in (b) by a domain wall coming from the Hall cross. Thus, the present observations indicate that several independent energy barriers (de-pinning centers) can

be involved also in the magnetization reversal at room temperature even though the Hall measurements presented in Fig. 1 can be described by a single energy barrier process. We attribute this to the different responses of the sample to the changes in the dynamics of the magnetic field application, namely 0.1 T/min during Hall measurements and $\sim 10^5$ T/min during Kerr observations[30]. This aspect of the magnetization reversal calls for a separate study which is beyond the scope of this work, nevertheless, it serves as evidence of the appearance of multiple reversal paths not only at low temperatures but also in room temperature fast switching experiments. This may play an important role in field-driven fast magnetization switching applications and is, therefore, in line for further investigation.

Studies in the literature have proposed different models to account for multiple switching probability sub-distributions. The 'alternative path'[16] model proposes that the initial state of a depinning process can evolve into the final state either in a direct manner or via an intermediate state leading to the observation of a switching probability distribution with more than one peak. Alternatively, the 'multiple injected domain wall'[28] model proposes a situation where the reversal can be driven by the propagation of domain walls injected in the system from different sources. Instead of an intermediate step between the initial and final states this model proposes multiple independent initial states with different statistics accounting for multiple peaks in the switching probability distribution. The measurements presented in this work suggest that the appearance of multiple peaks in the switching probability distributions can be related to different initial magnetization states generated at the moment when the initial magnetic field is applied. This is in agreement with the existence of multiple domain wall injection sources.

Longitudinal magneto-resistance measurements performed in a two-point configuration using the bias current probes (not shown) show that the magnetization reversal occurs in a single step, namely, that domain walls propagate freely during the magnetization reversal. However, since the domain walls reaching the Hall cross can also be generated outside the main Hall-bar channel the nature of the micro-magnetic event preceding the onset of propagation (nucleation or pinning) can not be unambiguously determined. Nevertheless, our findings regarding the existence of several processes acting in parallel giving rise to coercive field sub-distributions holds for both pinning and nucleation processes. Note that nucleation here refers to a reversal starting from a small preformed nucleus of non-saturated magnetization.

Domain nucleation has been shown to account for asymmetric magnetization reversal processes in other magnetic materials[29] where certain nucleation centers are active exclusively for one direction of the applied field, an effect attributed to domain wall chirality. In the cited work the asymmetric nucleation can be effectively suppressed by saturation at relatively low fields which is in agreement with the observations presented in this study. This scenario is compatible with the multiple injected domain wall model and constitutes a possible explanation for the observed coercive field asymmetry in our system. It is interesting to remark that asymmetric nucleation centers account

for the existence of asymmetric coercive field distributions with or without considering the presence of chirality-dependent pinning[31].
In conclusion, the existence of multiple switching probability sub-distributions and an asymmetric switching behaviour have been evidenced in FePt nanostructures. Both phenomena can be understood by considering that the selection between simultaneously available magnetization reversal paths does not happen in the vicinity of the coercive field but rather at the formation of the initial magnetization state under the saturation field. These findings have been related to an experimental realization of the multiple injected domain wall model.

Acknowledgments

We would like to thank S. Pizzini for valuable help during Kerr imaging and J. P. Attané for fruitful discussion. We gratefully acknowledge funding from the French National Research Agency (ANR) under the project ANR-2010-BLANC-1006-ELECMADE and from the Nanosciences Foundation of Grenoble. Device fabrication was carried out at the Plateforme Technologie Amont and Nanofab cleanroom facilities in Grenoble.

[1] R. F. C. Farrow, D. Weller, R. F. Marks, M. F. Toney, A. Cebollada, G. R. Harp, J. Appl. Phys. **79**, 5967 (1996).
[2] S. Okamoto, N. Kikuchi, O. Kitakami, T. Miyazaki, Y. Shimada, K. Fukamichi, Phys. Rev. B **66**, 024413 (2002).
[3] J. C. Lodder, L. T. Nguyen, *FePt Thin Films: Fundamentals and Applications.* In: Encyclopedia of Materials: Science and Technology. Elsevier, Amsterdam, pp. 1-10 (2005).
[4] S. B. Darling, S. D. Bader , J. Mater. Chem. **15**, 4189 (2005).
[5] A. Moser, K. Takano, D. T. Margulies, M. Albrecht, Y. Sonobe, Y. Ikeda, S. Sun, E. E. Fullerton, J. Phys. D: Appl. Phys. **35**, R157 (2002).
[6] K. Shibata, Mat. Trans. **44** Special Issue on L10-Type Ultra-High Density Magnetic Recording Materials, 1542 (2003).
[7] D. Weller, A. Moser, L. Folks, M. Best, W. Lee, M. Toney, M. Schwickert, J. Thiele, M. Doerner, IEEE Trans. Magn. **36**, 10 (2000).
[8] D. N. Lambeth, E. M. T. Velu, G. H. Bellesis, L. L. Lee, D. E. Laughlin, J. Appl. Phys. **79**, 4496 (1996).
[9] C. P. Luo, S. H. Liou, D. J. Sellmyer , J. Appl. Phys. **87**, 6941 (2000).
[10] M. Yu, M. F. Doerner, D. J. Sellmyer, IEEE Trans. Magn. **34**, 1534 (1998).
[11] C. Kim, T. Loedding, S. Jang, H. Zeng, Z. Li, Y. Sui, D. J. Sellmyer, Appl. Phys. Lett. **91**, 172508 (2007).
[12] J.-S. Noh, H. Kim, D. W. Chun, W. Y. Jeong, W. Lee, Current Applied Physics **11**, s33 (2011).
[13] O. Boulle, G. Malinowski, M. Kläui, Mat. Sci. Eng. R. **72**, 159 (2011).
[14] S. S. P. Parkin, M. Hayashi, L. Thomas, Science **320**, 190 (2008).
[15] D.A. Allwood, G. Xiong, C. Faulkner, D. Atkinson, D. Petit, R.P. Cowburn, Science **309**, 1688 (2005).
[16] J. P. Attané, D. Ravelosona, A. Marty, Y. Samson, C. Chappert , Phys. Rev. Lett. **96**, 147204 (2006).
[17] D. Halley, A. Marty, P. Bayle-Guillemaud, B. Gilles, J. P. Attané, Y. Samson, Phys. Rev. B **70**, 174438 (2004).

[18] The number of loops considered for each distribution at 300K, 200 K, and 100 K is 33, 72 and 75, respectively. All the distributions presented in this work correspond to the same magneto-transport device and the same Hall cross. At 300 K the measurement was stopped after 33 loops due to the irreversible loss of the Hall electrical connections. However, distributions of 100 loops at 300 K obtained from measurements on equivalent devices show the same type of single-peak switching probability.

[19] J. Vogel, J. Moritz, O. Fruchart, C. R. Physique **7** (2006).

[20] E. C. Stoner, E. P. Wohlfarth, Philos. Trans. London Ser. A **240**, 599 (1948).

[21] L. Néel, Ann. geophys. **5**, 99 (1949).

[22] G. Bayreuther, P. Bruno, G. Lugert, and C. Turtur, Phys. Rev. B **40**, 7399 (1989).

[23] J. Kurkijärvi, Phys. Rev. B **6**, 832 (1972).

[24] W. Wernsdorfer , PhD Thesis, Joseph Fourier University, Grenoble, (1996).

[25] W. Wernsdorfer, E. B. Orozco, K. Hasselbach, A. Benoit, B. Barbara, N. Demoncy, A. Loiseau, H. Pascard, D. Mailly , Phys. Rev. Lett. **78**, 1791 (1997).

[26] D. Givord, Q. Lu, F.P. Missell, M.F. Rossignol, D.W. Taylor, V. Villas Boas , J. Magn. Magn. Mater. **104-107**, 1129 (1992).

[27] D.W. Taylor, V. Villas-Boas, Q. Lu, M.F. Rossignol, F.P. Missell, D. Givord, S. Hirosawa , J. Magn. Magn. Mater. **130**, 225 (1994).

[28] J. Briones, F. Montaigne, M. Hehn, D. Lacour, J. R. Childress, M. J. Carey , Phys. Rev. B **83**, 060401(R) (2011).

[29] Y. L. Iunin, Y. P. Kabanov, V. I. Nikitenko, X. M. Cheng, D. Clarke, O. A. Tretiakov, O. Tchernyshyov, A. J. Shapiro, R. D. Shull, C. L. Chien , Phys. Rev. Lett. **98**, 117204 (2007).

[30] The device was placed at the center of a micro-coil generating 150 μs long magnetic field pulses of various intensities. The time delay between pulses was controlled manually and was of the order of 10 seconds. For a better visualization of the magnetic state an image of the fully switched state (after a saturating pulse of -300 mT for (a) and 300 mT for (b)) was subtracted from all the images taken after the field pulses. In each image, black (white) growing domains have oppositely oriented magnetizations with respect to the gray areas of the magnetic structure. The gray areas outside the structure correspond to the non-magnetic substrate. The field pulses preceding the acquisition of images (a) and (b) are +180 mT and -195 mT, respectively. The discrepancy between the coercive field values of the switching probability distributions and those of the pulse field experiments may be attributed to the uncertainty in determining the field values in the pulsed field experiment. This may be due to the position of the sample during the experiment which is situated at the surface and not inside the inner space of the coil where the fields values can be better estimated.

[31] L. K. Bogart, D. Atkinson, K. O'Shea, D. McGrouther, S. McVitie , Phys. Rev. B **79**, 054414 (2009).